Turkish Journal of Physics

http://journals.tubitak.gov.tr/physics/

Research Article

Turk J Phys
(2015) 39: 137 – 148

doi:10.3906/fiz-1409-30

Search for mixed-symmetry state in even-even $^{130-138}$Ce isotopes within the interacting boson model-2

Ali Mahdi Abdul HUSSAIN, Falih Hussain AL-KHUDAIR, Abdul Ridha Hussain SUBBER*
Department of Physics, College of Education for Pure Sciences, University of Basrah, Basrah, Iraq

Received: 27.09.2014 • **Accepted/Published Online:** 21.03.2015 • **Printed:** 30.07.2015

Abstract: The energy levels and reduced transition probabilities B(M1) and B(E2) of the even-even $^{130-138}$Ce isotopes were calculated by using the interacting boson model-2. We have analyzed the F-spin values and produced the symmetry labeling of the states. The calculated results were compared with the available experimental data. It was proved that the proton–neutron interacting boson model is a reasonable model for calculating low-lying spectra in the set of Ce isotopes and the quality of fit presented in this work is acceptable.

Key words: Ce isotopes, interacting boson model-2, mixed symmetry states, B(E2), B(M1)

1. Introduction

The atomic nuclei exhibit a variety of shapes, varying from spherical to gamma and soft to superdeformed and higher orders of deformation. Nuclei near the magic closed shell generally exhibit a spherical shape while nuclei having large numbers of bosons between the closed shells exhibit a deformation in their ground band. The possible shape of the nucleus may be deduced from microscopic calculations of the nuclear properties using a certain nuclear model. The even-even Ce isotopes lie in the transition region from γ-unstable to spherical shape, with the responsible O(6) to U(5) limit of the interaction boson model (IBM-1) [1]. The IBM-2 [2] suggests that the location of states of mixed (proton–neutron) symmetry is one of the most interesting open experimental and theoretical problems in the study of collective features of nuclei. This version shows the difference between proton and neutron boson wave functions and the states produced by IBM-2 contain all symmetry states with mixed-symmetry states, according to the U(6) representation [N-1, 1]. The quantity of proton–neutron symmetry of each state is identified by a new quantum number called F-spin [3]. Such states can be thought of as states in which the proton and neutron oscillate out of phase with respect to one another.

The excitation energies of collective quadrupole excitations in nuclei near the magic closed shell depend on the number of nucleons outside the closed shell. In the even-even cerium isotopes the number of neutron boson N_ν outside the closed shell varies from 5 in ^{130}Ce to 1 for ^{138}Ce, while the number of proton bosons is equal to 4 for all isotopes. The energy ratios $E4_1^+/E2_1^+$ experimentally equal 2.806, 2.640, 2.562, 2.380, and 2.317, respectively. For model limits, the typical values are 2.0, 2.5, and 3.3 for the U(5), O(6), and SU(3) limits, respectively [4].

The one-quadruple phonon states at around 2 MeV have been recognized as a good candidate to be the first mixed-symmetry state $2^+_{1,ms}$ and have been studied systematically as O(6) nuclei [4,5]. These states have

*Correspondence: dabrhs@hotmail.com

been found in Xe, Ba, and Ce nuclei with mass numbers around A = 130 and they are a good clarification of the O(6) dynamical symmetry [6]. The mixed symmetry states have the following signatures [7]:

1. The one-phonon $2^+_{1,ms}$ state is the lowest MSS in the vibrational nuclei.
2. The $2^+_{1,ms}$ state decay to the 2^+_1 state by large M1 matrix elements $\approx 1\ \mu_N$ and this is the most important signature ($\langle 2^+_{1,ms}|T(M1)|2^+_1\rangle \approx 1\mu_N$).
3. A relatively weak collective E2 transition strength of a few W.u. units for the $2^+_{1,ms} \rightarrow 0^+_1$ transition.
4. Small value of the mixing ratio δ(E2/M1) for transition from $2^+_{1,ms}$ to the 2^+_1.

A number of experimental and theoretical studies of even-even Ce isotopes have been reported, like studying the shape and recognizing the deformation in ^{130}Ce and ^{132}Ce nuclei [8,9]. The measurement of the magnetic moment and the identification of the first mixed symmetry state in ^{134}Ce and ^{136}Ce have also been reported [10–13]. The backbending in the even-even Ce isotopes using the truncated shell model was studied in [14]. The structure of low-lying states of these isotopes using the IBM and the microscopic IBM calculation was investigated in [15–19].

The aim of this study is to discuss the structure of cerium isotopes from A = 130 to A = 138 in the framework of the IBM-2. The work contains the calculation of the energy levels, electromagnetic transition probabilities, mixing ratios, and determination of the mixed-symmetry states employing the effect of changing the Majorana parameters on the energies and reduced transition probabilities.

2. Interaction boson model (IBM-2)

The general IBM-2 Hamiltonian can be written as [20]:

$$H = H_\pi + H_\upsilon + H_{\pi\upsilon}, \tag{1}$$

where H_π and H_υ are the proton and neutron parts and $H_{\pi\upsilon}$ is the interaction between them.

The Hamiltonian generally used in phenomenological calculations can be written as:

$$H = \varepsilon_d\left(\hat{n}_{d_\pi} + \hat{n}_{d\upsilon}\right) + \kappa_{\pi,\upsilon}\left(\hat{Q}_\pi.\hat{Q}_\upsilon\right) + \hat{M}_{\pi\upsilon} + \hat{V}_{\pi\pi} + \hat{V}_{\upsilon\upsilon}, \tag{2}$$

where quadrupole–quadrupole interaction between neutrons and protons with strength $\kappa_{\pi\upsilon}$ is:

$$\hat{Q}_\rho = \left[d^+_\rho \times \tilde{s}_\rho + s^+_\rho \times \tilde{d}_\rho\right]^{(2)} + \chi_\rho\left[d^+_\rho \times \tilde{d}_\rho\right]^{(2)}. \tag{3}$$

The Majorana term is:

$$\hat{M}_{\nu\pi} = \frac{1}{2}\xi_2[s^+_\nu d^+_\pi - d^+_\nu s^+_\pi]^{(2)}.[s_\nu d_\pi - d_\nu s_\pi]^{(2)} - \sum_{k=1,3}\xi_k[d^+_\nu d^+_\pi]^{(k)}.[d_\nu d_\pi]^{(k)}. \tag{4}$$

The interaction of like bosons is given in the following form:

$$\hat{V}_{\rho\rho} = \frac{1}{2}\sum_{(L=0.2.4)} c_{L\rho}\left[d^+_\rho d^+_\rho\right]^{(L)}.\left[\tilde{d}_\rho \tilde{d}_\rho\right]^{(L)} \tag{5}$$

where $\rho = \pi\nu$, ε_d is the energy difference between (s) and (d) bosons, and $\hat{n}_{d\rho}$ is the number of (d-boson) operators. The E2 transition probability operator in the IBM-2 is given as [5]:

$$\hat{T}\,(E2) = e_\pi \hat{Q}_\pi + e_\upsilon \hat{Q}_\upsilon, \tag{6}$$

where e_π and e_υ are boson effective charges depending on the boson number. The M1 transition probability operator can be written as [5]:

$$\hat{T}\,(M1) = \left[\frac{3}{4\pi}\right]^{1/2} \left(g_\pi \hat{L}_\pi + g_\upsilon \hat{L}_\upsilon\right), \tag{7}$$

where $\hat{L}_\rho = \sqrt{10}\left[d_\rho^+ \times \tilde{d}_\rho\right]^{(1)}$ is the angular momentum operator of each boson, and g_π and g_υ are the g-factors for the proton and neutron bosons, respectively.

3. Calculation and results

3.1. Energy levels

For even-even cerium isotopes Z = 58 and neutron number varying between N = 72 and N = 80, according to closed shells Z = 50 and N = 82, the proton boson is of a particle type while, the neutron boson is a hole type. The best fitting parameters used in the NPBOS code [21] to obtain the low-lying energy levels are given in Table 1. From this table, one can see that $C_{0\nu} = C_{2\nu} = C_{4\nu} = 0$. The values of $C_{0\pi} = -0.3$ MeV, $C_{4\pi} = 0.3MeV$, and $\chi_\nu = -\chi_\pi = 0.90$ hold for all isotopes[22]. The choice of the parameter $\chi_\nu = -\chi_\pi$ underscores the belonging to the O(6) limit, plus the ratio $E(4_1^+)/E(2_1^+)$, which is shown in Figure 1. The parameter ε_d is varied with decreasing number of neutron bosons, while $\kappa_{\pi\nu}$ is changed with increasing mass number. Figure 2 presents the smooth variation of these important parameters used in the calculation (ε_d and $\kappa_{\pi\nu}$) as a function of neutron number. The Majorana parameters used are $\xi_1 = 0.3$MeV and $\xi_3 = -0.1$ MeV, fixed for all isotopes, while the ξ_2 parameter was adjusted to fit the $2^+$and 1^+ mixed-symmetry states. The parameters are chosen to give the best fit with the available experimental data, especially those of the mixed-symmetry states and high energy states, in comparison with those parameters used in [19].

Table 1. The parameters of the IBM-2 Hamiltonian. $x_\nu = -x_\pi = 0.9$, $C_{0\nu} = C_{2\nu} = C_{4\nu} = 0$ have been chosen for $^{130-138}$Ce isotopes, and all parameters are in MeV units except x_ν and x_π, which are unitless.

A	$\varepsilon_{\mathbf{d}}$	$\kappa_{\pi\nu}$	$\xi_{\mathbf{1}}$	$\xi_{\mathbf{2}}$	$\xi_{\mathbf{3}}$	$\mathbf{C_{0\pi}}$	$\mathbf{C_{2\pi}}$	$\mathbf{C_{4\pi}}$
130	0.35	–0.230	0.300	0.300	–0.100	–0.300	0.300	0.300
132	0.45	–0.230	0.300	0.010	–0.100	–0.300	0.300	0.300
134	0.65	–0.190	0.300	0.170	–0.100	–0.300	0.300	0.300
136	0.85	–0.160	0.300	0.250	–0.100	–0.300	–0.300	0.300
138	0.90	–0.100	0.300	0.600	–0.100	–0.300	–0.300	0.300

A comparison between experimental energy levels and the IBM-2 calculations is presented in Figures 3. We notice that for the ^{130}Ce isotope the calculated energy of the 0_2^+ state (two-phonon triplet) is equal to 0.823 MeV, while the experimental value is equal to 1.025 MeV (the difference is 0.202 MeV), and the calculated energy value of the 2_2^+ state is 0.571 MeV, while the experimental value is 0.834 MeV. We would like to mention that all the calculated ground band states are close to the experimental data. The same case holds for the ^{132}Ce isotope, where the maximum difference between the energies is 0.169 MeV. The backbending phenomenon is clear in the ^{134}Ce isotope [16].

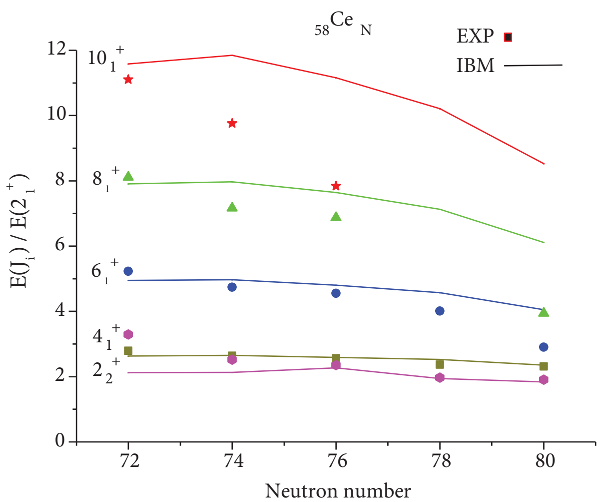

Figure 1. Comparison between calculated and experimental values of the $[\mathbf{E(J_i^+)/E(2_1^+)}]$ ratio in $^{\mathbf{A}}_{\mathbf{58}}\mathbf{Ce}$ isotopes.

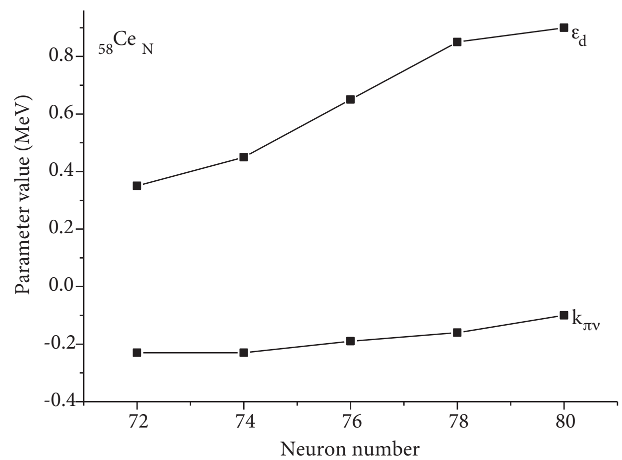

Figure 2. The parameters used in the calculations as a function of neuron number in $^{\mathbf{A}}_{\mathbf{58}}\mathbf{Ce}$ isotopes.

3.2. Mixed-symmetry states

The mixed symmetry states originate from a mixture of two wave functions for the proton and neutron. These states have two distinguishable decay features, one a strong M1 and another a weak decay to the ground state. The rapid influence on the energy of these states by changing the Majorana parameters, especially ξ_2, gives an indication of the mixing. The amount of mixing in the proton and neutron wave function can be recognized by the ratio R, which is calculated by [23]:

$$R = \frac{\langle J|F^2|J\rangle}{F_{max}\,(F_{max}+1)}. \tag{8}$$

Our attention is especially drawn to the $(F = F_{max})$ and $(F = F_{max} - 1)$ states, where:

$$F_{max} = \frac{(N_\pi + N_\nu)}{2}. \tag{9}$$

We can suppose states that are written as:

$$|\,J\rangle = \alpha|\,F_{max}\rangle + \beta|\,F_{max}-1\rangle\,, \quad \alpha^2+\beta^2 = 1. \tag{10}$$

It is simple to calculate

$$\langle J|F^2|J\rangle = \alpha^2 F_{max}(F_{max}+1) + \beta^2(F_{max}-1)F_{max}, \tag{11}$$

where α and β are important to measure the amount of mixed symmetry in each state.

The lowest mixed-symmetry state in the O(6) nuclei corresponds to the 2^+ state at energy close to 2 MeV, and we can see that the 2_3^+ state represents the lowest mixed symmetry in $^{132-136}$Ce isotopes; these states

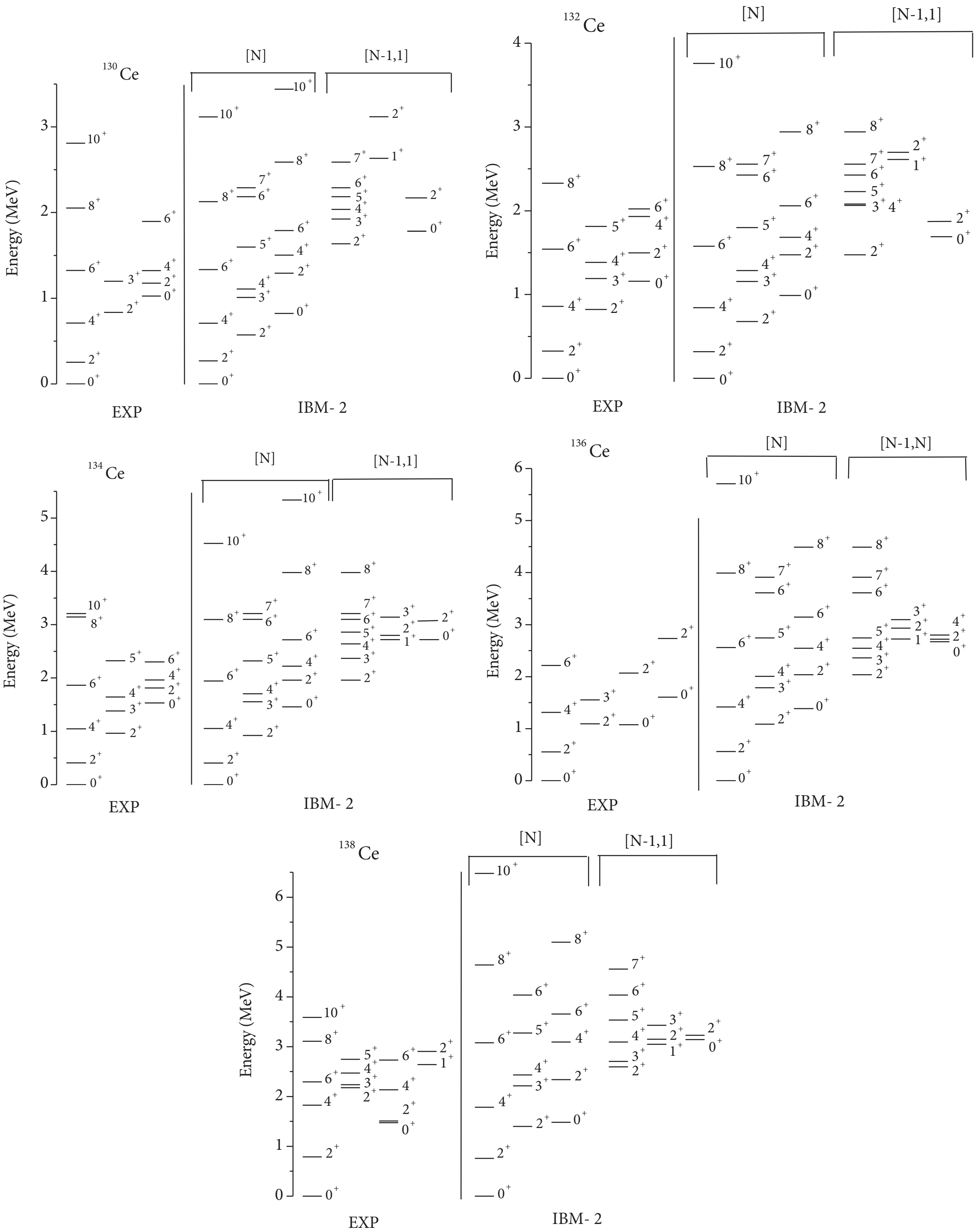

Figure 3. Comparison between calculated energy levels and experimental data for $^{A}_{58}\mathbf{Ce}$ isotopes.

have energies of 1.475 MeV, 1.96 MeV, and 2.036 MeV, respectively. The 2_4^+ state is of mixed symmetry in ^{130,138}Ce isotopes at energy of 1.635 MeV and 2.594 MeV, respectively. It is remarkable to see the presence of the 2^+ MSS at energies of less than 2 MeV, which is the property of the O(6) region around A = 130, and these values are in good agreement with the experimental data [24]. The values of the ratio R in the mixed-symmetry states for the set of isotopes are shown in Figure 4.

The 1_1^+ state has a mixed-symmetry character through the excitation energies calculated for the studied set of isotopes of 2.633, 2.745, 2.721, 2.723, and 3.050 MeV, respectively. The influence of changing the ξ_2 parameter on the 2^+ states is presented in Figure 5. It is clear from this figure that states that have mostly mixed-symmetry characters are strongly influenced by variation of the ξ_2 parameter. In the ^{134}Ce nucleus, there are two states, 2_3^+ and 2_4^+, separated by energy of 0.156 MeV, and the investigation of these states is very important for recognizing the lowest mixed-symmetry states [25]. The same case is true in the ^{136}Ce nucleus; the difference between two energies was 0.091 MeV, despite the 2_4^+ state not being of mixed symmetry according to the value of the R ratio.

3.3. Electromagnetic transitions

In the IBM-2, the E2 transition operator is given by [4,5]:

$$\hat{T}\,(E2) = e_\pi \hat{Q}_\pi + e_\upsilon \hat{Q}_\upsilon. \tag{12}$$

Here, e_π and e_υ are the effective boson charges for the proton and neutron, respectively. We obtained these values from the experimental data of B(E2:$2_1^+ \rightarrow 0_1^+$), according to the following relative to the O(6) limit [26]:

$$B\left(E2:\, 2_1^+ \rightarrow 0_1^+\right) = \frac{(N+4)(e_\pi N_\pi + e_\nu N_\nu)}{5N}. \tag{13}$$

By using the method from [27], a plot between $M = N_\pi^{-1}[5N(N+4)^{-1}B\,(E2;2_1 \rightarrow 0_1)]^{\frac{1}{2}}eb$ and the $\frac{N_\nu}{N_\pi}$ ratio has been created, as shown in Figure 6. The slope of the best-fitting straight line is $e_\upsilon = 0.15\,eb$ and the intercept is $e_\pi = 0.10\,eb$.

The M1 transition operator can be written as [28]:

$$\hat{T}\,(M1) = \left[\frac{3}{4\pi}\right]^{1/2}\left(g_\pi \hat{L}_\pi + g_\upsilon \hat{L}_\upsilon\right),\quad \hat{L}_\rho = \sqrt{10}\left[d_\rho^+ \times \tilde{d}_\rho\right]^{(1)} \tag{14}$$

where g_π and g_υ are the boson g-factors for the proton and neutron, respectively, and $\hat{L}_\rho$ is the angular momentum operator. The mixing ratio is considered as a ratio of E2 and M1 matrix elements strength, written as [28]:

$$\delta\left(\frac{E2}{M1}\right) = 0.835\,E_\gamma \Delta\left(\frac{eb}{\mu_N}\right)\ where \Delta = \frac{\langle I_f|T^{E2}|I_i\rangle}{\langle I_f|T^{M1}|I_i\rangle} \tag{15}$$

To calculate the M1 reduced transition probability B(M1), values of $g_\pi = 1$ and $g_\upsilon = 0$ have been used to obtain the best agreement with the experimental data taken from [11,12]. The calculated values for B(E2) and B(M1) reduced transition probability are given in Tables 2 and 3.

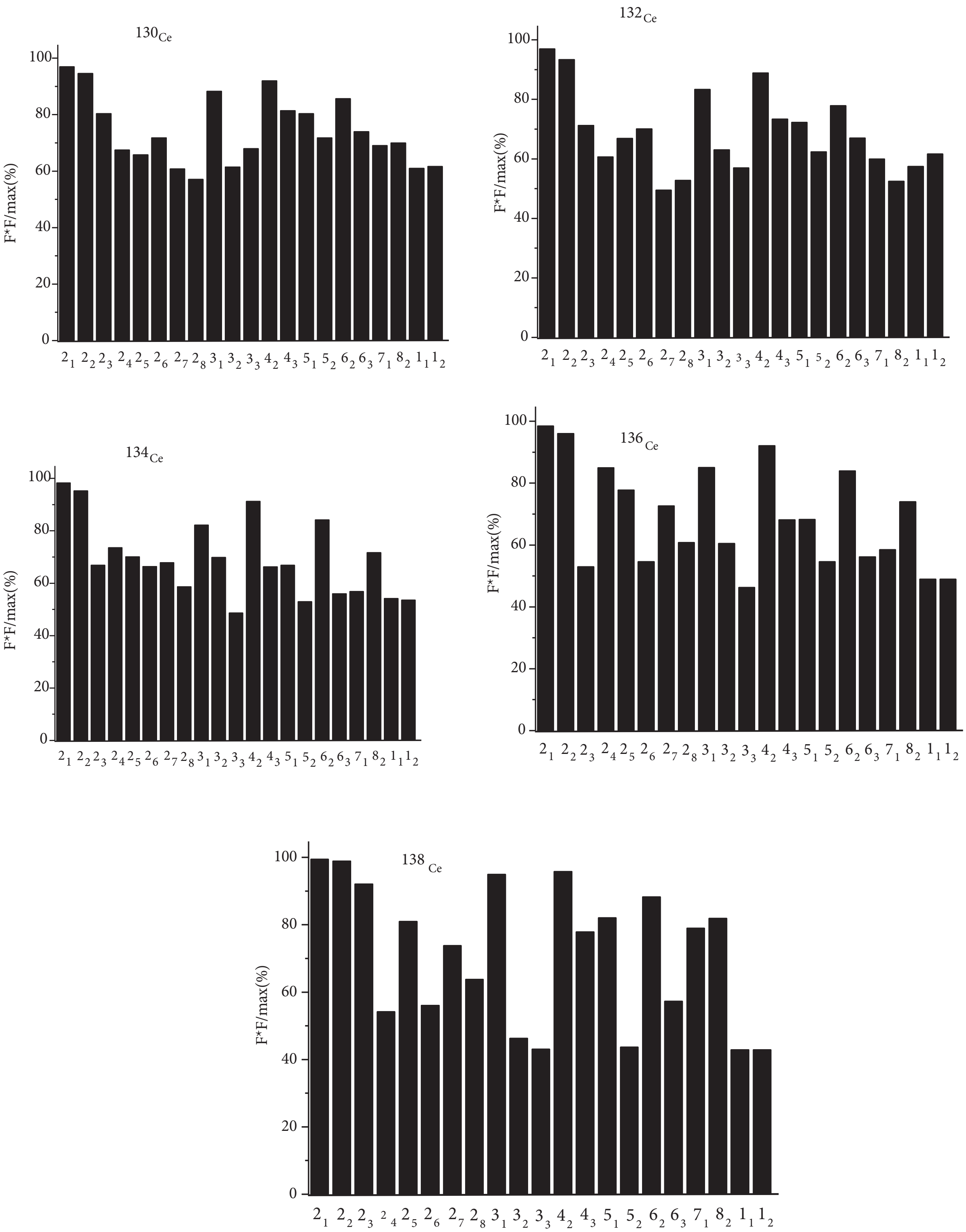

Figure 4. The R-values of low-lying states in IBM-2 for Ce isotopes.

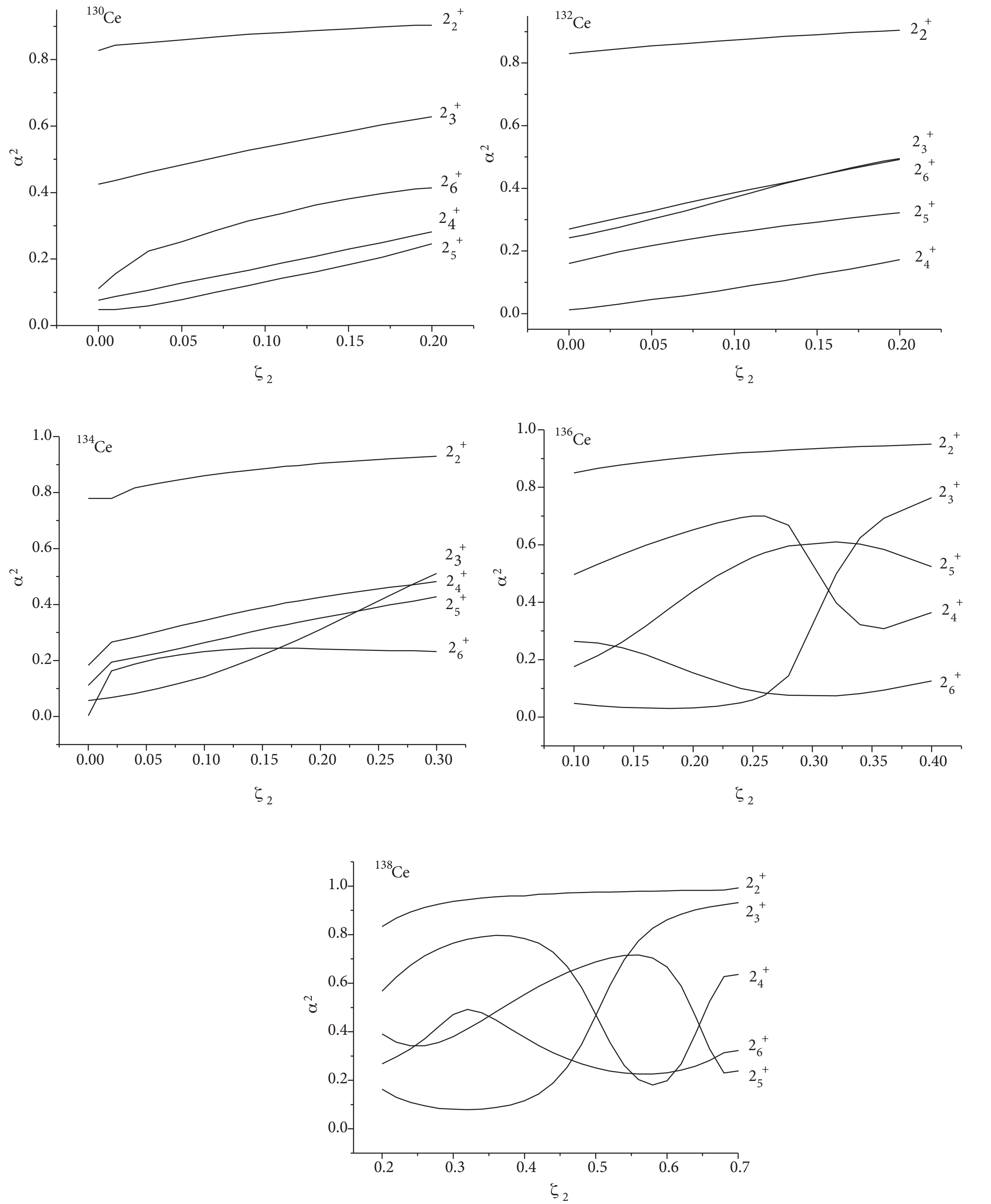

Figure 5. Amplitude squared of ($\mathbf{F} = \mathbf{F}_{\max}$) component of ($\mathbf{2^+_{ms}}$) and ($\mathbf{2^+_i}$) states as a function of Majorana parameter (ξ_2).

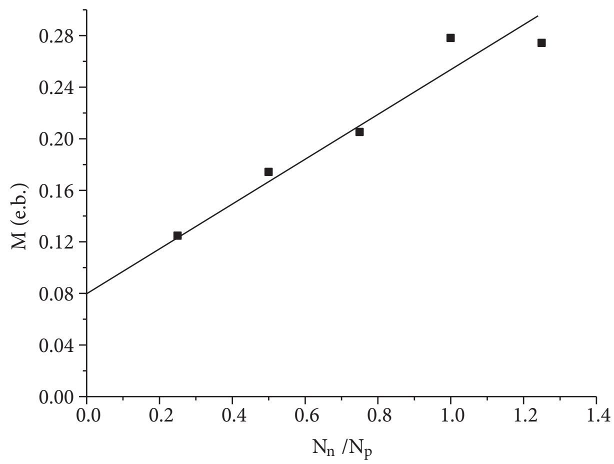

Figure 6. The $M = N_\pi^{-1}[5N(N+4)^{-1}B\,(E2;2_1 \rightarrow 0_1)]^{\frac{1}{2}}eb$ values as a function of the ratio $(\frac{N_\nu}{N_\pi})$.

Table 2. Experimental and calculated B(E2) (in unit e^2b^2) and B(M1) (in unit μ_N^2) for $^{130-134}$Ce isotopes.

$J_i^+ \rightarrow J_f^+$	$^{130}_{58}Ce$			$^{132}_{58}Ce$			$^{134}_{58}Ce$		
	B(E2)		B(M1)	B(E2)		B(M1)	B(E2)		B(M1)
	Exp.	IBM	IBM	Exp.	IBM	IBM	Exp.	IBM	IBM
$2_1^+ \rightarrow 0_1^+$	0.3480	0.379		0.3711	0.2955		0.2117	0.2114	
$2_2^+ \rightarrow 2_1^+$		0.4610	0.0409		0.3695	0.0571		0.2908	0.0037
$2_3^+ \rightarrow 2_1^+$		0.0001	0.0048		0.0004	0.0161		0.0001	0.0834
$2_4^+ \rightarrow 2_1^+$		0.0001	0.0089		0.0001	0.0081		0.0001	0.0438
$2_5^+ \rightarrow 2_1^+$		0.0002	0.0437		0.0005	0.0838		0.0001	0.1615
$2_4^+ \rightarrow 2_2^+$		0.0005	0.0170		0.0036	0.0244		0.0079	0.0174
$2_5^+ \rightarrow 2_2^+$		0.0025	0.0075		0.0040	0.0004		0.0014	0.0043
$3_1^+ \rightarrow 2_1^+$		0.0057	0.0013		0.0026	0.0020		0.0001	0.0007
$3_1^+ \rightarrow 4_1^+$		0.1192	0.0380		0.0969	0.0597		0.09	0.0724
$3_2^+ \rightarrow 2_1^+$		0.0001	0.0003		0.0001	0.0008		0.0006	0.0010
$3_2^+ \rightarrow 2_2^+$		0.0009	0.0410		0.0044	0.0608		0.0084	0.1211
$4_1^+ \rightarrow 2_1^+$	0.6530	0.5216		0.4110	0.4011		0.1587	0.2862	
$4_2^+ \rightarrow 2_1^+$		0.0074			0.0044			0.0001	
$4_2^+ \rightarrow 2_2^+$		0.2973			0.2204			0.1616	
$4_2^+ \rightarrow 3_1^+$			0.0273			0.0256			0.0563
$5_1^+ \rightarrow 4_1^+$		0.0092	0.0081		0.0044	0.0106		0.0001	0.0029
$6_1^+ \rightarrow 4_1^+$	0.7469	0.5539		0.5587	0.4187		0.0570	0.3020	
$8_1^+ \rightarrow 6_1^+$	1.1340	1.0987		0.2713	0.3767		0.0987	0.2811	
$1_1^+ \rightarrow 2_1^+$		0.0001	0.0847		0.0003	0.0019		0.0016	0.0103
$1_1^+ \rightarrow 2_2^+$		0.0009	0.0992		0.0026	0.3031		0.0001	0.4177

The 2_3^+ state was indicated as the lowest mixed state $2_{1,ms}^+$ in $^{132-136}$Ce isotopes (two-phonon), which decays to the 2_1^+ state for an enhanced M1 transition with matrix elements 1.3, 1.3, and 1.2, respectively [4]. This is in agreement with the forecast of the IBM-2 for the two-phonon mixed-symmetry states, while the 2_4^+ state representing the $2_{1,ms}^+$ in ^{130,138}Ce isotopes has matrix elements of 1.3 and 1.07, respectively.

In the ^{138}Ce isotope, we notice the calculated value for transition strength of [B(M1:$2_4^+ \rightarrow 2_1^+$) = 0.14 μN], while its experimental value is 0.122 μN, and M1 matrix elements are [$\langle 2_1^+|M1|2_4^+\rangle = 1.09$]. The

$2^+_{3,4}$ states give the total M1 strength $[\sum B\left(M1 : 2^+_{3,4} \rightarrow 2^+_1\right) = 0.17\mu N]$, and this is in agreement with the calculation of ^{136}Ba as an O(6) nucleus in [29]. The separation energy of these states is about 0.254 MeV.

Table 3. Experimental and calculated B(E2) (in unit e^2b^2) and B(M1) (in unit μ_N^2) for ^{136,138}Ce isotopes.

$J_i^+ \rightarrow J_f^+$	$^{136}_{58}Ce$				$^{138}_{58}Ce$			
	B(E2)		B(M1)		B(E2)		B(M1)	
	Exp.	Cal.	Exp.	Cal.	Exp.	Cal.	Exp.	Cal.
$2_1^+ \rightarrow 0_1^+$	0.1619	0.1327			0.0897	0.0743		
$2_2^+ \rightarrow 0_1^+$	0.0022	0.0001				0.0		
$2_2^+ \rightarrow 2_1^+$	0.1993	0.1935	0.0010	0.0196	0.1185	0.1128		0.0025
$2_3^+ \rightarrow 2_1^+$	0.0032	0.0016	0.025	0.1690	0.0317	0.0003	0.058	0.0306
$2_4^+ \rightarrow 2_1^+$	0.0166	0.0002	0.16	0.0431	0.0027	0.0041	0.122	0.1488
$2_5^+ \rightarrow 2_1^+$		0.0013		0.0363		0.0008	≤ 0.06	0.0545
$2_4^+ \rightarrow 2_2^+$	0.456	0.0095	00.644	0.0001		0.0001		0.0099
$2_5^+ \rightarrow 2_2^+$		0.0039		0.0409		0.0004		0.0058
$3_1^+ \rightarrow 2_1^+$		0.0006		0.0005		0.0001		0.0002
$3_1^+ \rightarrow 4_1^+$		0.0669		0.0489		0.040		0.0101
$3_2^+ \rightarrow 2_1^+$		0.0019		0.0021		0.0016		0.0002
$3_2^+ \rightarrow 2_2^+$		0.0020		0.1115		0.0005		0.1271
$4_1^+ \rightarrow 2_1^+$	0.0332	0.1863				0.110		
$4_2^+ \rightarrow 2_1^+$		0.0001				0.0001		
$4_2^+ \rightarrow 2_2^+$		0.1111				0.0648		
$4_2^+ \rightarrow 3_1^+$				0.0380				0.0078
$5_1^+ \rightarrow 4_1^+$		0.0005		0.0001		0.0001		0.0002
$6_1^+ \rightarrow 4_1^+$		0.1962				0.1156		
$8_1^+ \rightarrow 6_1^+$		0.1761				0.0968		
$1_1^+ \rightarrow 2_1^+$		0.0013		0.0224		0.0011		0.0035
$1_1^+ \rightarrow 2_2^+$		0.0016		0.1790		0.0039		0.1840

In the selection of $2^+_{2,ms}$ states, we depend on the strong M1 decay to the symmetry 2^+_2 two-phonon state, in ^{130}Ce nucleus, and the 2^+_5 state is considered as the $2^+_{2,ms}$ state because it has [B(M1:$2^+_5 \rightarrow 2^+_2$)=0.0075 μN] where M1 $>$ E2. In $^{132-134}$Ce isotopes the 2^+_4 state is $2^+_{2,ms}$ and it decays to the 2^+_2 state by a strong M1; these states have B(M1) equal to 0.0244 , 0.0744 μ_N , while B(E2) is equal to 0.0036, 0.0079 e^{2}b^2, respectively. For the ^{136}Ce nuclei, the 2^+_5 state is considered as $2^+_{2,ms}$ through the R value equal to 77.8 having B(M1) = 0.0409 μN where M1 $>$ E2, while the 2^+_4 state is not of mixed-symmetry state because the M1 decay is weak, E2 $>$ M1, and R = 85%. In the ^{138}Ce nucleus, the 2^+_5 state is not of mixed symmetry because the M1 decay is weak and R = 81%. The 2^+_6 state does not have comprehensive properties of mixed symmetry because the M1 decay is weak. We notice that the 3^+_1 state is the fully symmetric state for all isotopes, while the 3^+_2 state is of mixed symmetry at energy values between 1.925 and 2.706 MeV. The calculated mixing ratio compared with experimental values is shown in Table 4. The results show that there are several disagreements in value and sign despite the agreement in some cases. However, it is a ratio between very small quantities and any change in the dominator will have influence on the value. We notice that the large calculated values are not due to a dominant E2 transition, but it is under the effect of a very small M1 component in the transition.

Table 4. Experimental and calculated values for mixing ratio (δ) for $^{130-138}$Ce isotopes.

$J_i^+ \to J_f^+$	$^{130}_{58}Ce$		$^{132}_{58}Ce$		$^{134}_{58}Ce$		$^{136}_{58}Ce$		$^{138}_{58}Ce$	
	Exp.	Cal.	Exp.	Cal.	Exp.	Cal.	Exp.	Cal.	Exp.	Cal.
$2_2^+ \to 2_1^+$		– 0.84	9	– 0.76	9	– 1.21		1.33	–1.97	– 3.54
$2_3^+ \to 2_1^+$		0.08	–1.4	0.15		0.02		– 0.12	–0.83	– 0.15
$2_4^+ \to 2_1^+$		– 0.03	–0.08	0.16		0.07		0.09	0.18	– 0.25
$2_5^+ \to 2_1^+$		0.11		0.11		0.006		– 0.29		– 0.20
$2_4^+ \to 2_2^+$		– 0.16	–0.28	– 0.35		– 0.67		– 12.8		0.13
$2_5^+ \to 2_2^+$		0.68		3.06		– 0.68		– 0.34		– 0.29
$3_1^+ \to 2_1^+$		– 1.27	4.8	– 0.79	4	0.08		– 1.15		– 0.62
$3_1^+ \to 4_1^+$		– 0.44	2.6	– 0.33		– 0.46		– 0.36		– 0.71
$3_2^+ \to 2_1^+$		– 0.67		0.32		– 0.12		1.42		4.29
$3_2^+ \to 2_2^+$		0.16		0.31		– 0.96		0.14		– 0.06
$5_1^+ \to 4_1^+$		– 0.78		– 0.51	1.86	0.04		– 2.45		– 0.66
$1_1^+ \to 2_1^+$		0.05		0.76		– 0.76		– 0.44		– 1.07
$1_1^+ \to 2_2^+$		0.16		0.14		0.02		– 0.13		– 1.20

3.4. Concluding remarks

In summary, we have investigated the level structure and electromagnetic transition of even-even $^{130-138}$Ce isotope chains by using the proton–neutron IBM. Using the F-spin values, mixed-symmetry state types, one- and two-phonon states $J^\pi = 2^+$, have been identified. The two-phonon mixed-symmetry states 1^+ and 3^+ were identified also. The effect of the Majorana parameter ξ_2 on the position of the mixed-symmetry states in the energy spectrum was discussed in detail. The fast M1 decay identifies the 2_3^+ state to be the first 2^+ mixed symmetry state near 2 MeV in A = 130 to A = 134 isotopes, while the 2_4^+ are the mixed-symmetry 2^+ states in A = 136 and A = 138. The IBM-2 results support the mixed-symmetry phenomenon for the multiphonon structure in these isotopes.

Acknowledgment

The authors would like to thank the Physics Department and the College of Education for Pure Sciences for their financial support and encouragement.

References

[1] Pascu, S.; Zamfir, N. V.; Cata-Danil, G.; Marginean, N. *Phys. Rev.* **2010**, *C81*, 1–9.

[2] Arima, A.; Iachello, F. *Adv. Nucl. Phys.* **1987**, *13*, 139–165.

[3] Osuka, T.; Arima, A.; Iachello, F. *Nucl. Phys. A* **1978**, *309*, 1–33.

[4] Arima, A.; Iachello, F. *The Interaction Boson Model*; Cambridge University Press: Cambridge, UK, 1987.

[5] Iachello, F.; *Phys. Rev. Lett.* **1984**, *53*, 1427–1429.

[6] Casten, R. F.; Von Brentano, P. *Phys. Lett.* **1985**, *152*, 22–25.

[7] Pietralla, N.; Fransen, C.; Von Brentano, P.; Dewald, A.; Fitzler, A.; Friebner, C.; Gableske, J. *Phys. Rev. Lett.* **2000**, *84*, 3775–3778.

[8] Wilson, J. N.; Boll, G. C.; Drake, T. E.; Flibotte, S.; Galindo-Uribarri, A.; de Graff, J.; Hackman, G.; Mullins, S. M.; Nieminen, J. M.; Janzen, V. P. et al. *Phys. Rev.* **1997**, *C55*, 519–520.

[9] Kirwan, A. J.; Ball, G. C.; Bishop, P. J.; Godfrey, M. J.; Nolan, P. J.; Thornley, D. J.; Love, D. J. G.; Nelson, A. H. *Phys. Rev. Lett.* **1987**, *58*, 467–470.

[10] Zemel, A. PhD, Weizmann Institute of Science, Rehovot, Israel, 1981.

[11] Ahn, T.; Rainovski, G.; Pietralla, N.; Coquard, L.; Moller, T.; Costin, A.; Janssens, R. V. F.; Lister, C. J.; Carpenter, M. P.; Zhu, S. *Phys. Rev.* **2012**, *C86*, 1–7.

[12] Rainovski, G.; Pietralla, N.; Ahn, T.; Lister, C. J.; Janssens, R. V. F.; Carpenter, M. P.; Zhu, S.; Barton, C. J. *Phys. Rev. Lett.* **2006**, *96*, 1–4.

[13] Ahn, T.; Pietralla, N.; Rainovski, G.; Costin, A.; Dusling, K.; Li, T. C.; Linnemann, A.; Pontillo, S. *Phys. Rev.* **2007**, *C75*, 1–7.

[14] Tazoe, H.; Obata, H.; Gamo, T. *J. Anal. At. Spectrum* **2007**, *22*, 616–622.

[15] Lakshmi, S.; Jain, H. C.; Joshi, P. K.; Jain, A. K.; Malik, S. S. *Phys. Rev.* **2004**, *C69*, 1–8.

[16] Takahashi, T.; Yoshinaga, N.; Higashiyama, K. *Phys. Rev.* **2007**, *C71*, 1–9.

[17] Al-Hilfy, A.; Al-Khudair, F. H.; Al-Asadi, J. M. *Journal of Basrah Researcher* **2013**, *39*, 171–177.

[18] Pietralla, N.; Rainovski, G.; Ahn, T.; Carpenter, M. P.; Janssens, R. V. F.; Lister, C. J.; Zhu, S. *Capture Gamma-Ray Spectroscopy and Related Topics*; American Institute of Physics: College Park, MD, USA, 2006.

[19] Turkan, N.; Maras, I. *Indian Academy of Sciences*, **2007**, *68*, 769–778.

[20] Gade, A.; Wiedenhover, I.; Gableske, J.; Gelberg, A.; Meise, H.; Pietralla, N.; Von Brentano, P. *Nucl. Phys. A* **2000**, *665*, 268–284.

[21] Otsuka, T.; Yoshida, N. Program NPBOS, Japan Atomic Energy Research Institute Report JAERI – M85 – 094, 1985.

[22] Scholten, O.; Heyde, K.; Van Isacker, P.; Jolie, J.; Moreau, J.; Waroquier, M. *Nucl. Phys. A* **1985**, *438*, 41–77.

[23] Giannatiempo, A.; Nannini, A.; Sona, P.; Cutiou, D. *Phys. Rev.* **1995**, *C52*, 2969–2983.

[24] Wiedenhover, I.; Gelberg, A.; Otsuka, T.; Pietralla, N.; Gableske, J.; Dewald, A.; Von Brentano, P. *Phys. Rev.* **1997**, *C56*, R2354–2357.

[25] Al-Khudair Falih, H.; Li, Y. S.; Long, G. L. *J. Phys. G Nucl. Part. Phys.* **2004**, *30*, 1287–1298.

[26] Van Isacker, P.; Heyde, K.; Jolie, J.; Sevrin, A. *Ann. Phys.* **1986**, *171*, 253–296.

[27] Subber, A. R. H. PhD, University of Sussex, Sussex, UK, 1987.

[28] Hamilton, W. D.; Irback, A.; Elliott, J. P. *Phys. Rev. Lett.* **1984**, *53*, 2469–2472.

[29] Pietralla, N.; Belic, D.; Von Brentano, P.; Fransen, C.; Herzberg, R. D.; Kneissl, U.; Maser, H.; Matschinsky, P.; Nord, A.; Otsuka, T. et al. *Phys. Rev.* **1998**, *C58*, 796–800.